



HAL
open science

High-order finite elements in tokamak free-boundary plasma equilibrium computations

Francesca Rapetti, Blaise Faugeras, Cedric Boulbe

► **To cite this version:**

Francesca Rapetti, Blaise Faugeras, Cedric Boulbe. High-order finite elements in tokamak free-boundary plasma equilibrium computations. 2021. hal-03423469v1

HAL Id: hal-03423469

<https://hal.science/hal-03423469v1>

Preprint submitted on 10 Nov 2021 (v1), last revised 6 Oct 2023 (v3)

HAL is a multi-disciplinary open access archive for the deposit and dissemination of scientific research documents, whether they are published or not. The documents may come from teaching and research institutions in France or abroad, or from public or private research centers.

L'archive ouverte pluridisciplinaire **HAL**, est destinée au dépôt et à la diffusion de documents scientifiques de niveau recherche, publiés ou non, émanant des établissements d'enseignement et de recherche français ou étrangers, des laboratoires publics ou privés.

High-order finite elements in tokamak free-boundary plasma equilibrium computations

Francesca Rapetti, Blaise Faugeras and Cedric Boulbe

Abstract We wish to compute numerically the equilibrium for a hot plasma in a tokamak. For such a problem in an axisymmetric configuration, we present a non-overlapping mortar element approach, that couples piece-wise linear finite elements in a region that does not contain the plasma and reduced Hsieh-Clough-Tocher finite elements elsewhere, to approximate the magnetic flux field on a triangular mesh of the poloidal tokamak section. This approach has the flexibility to achieve easily and at low cost higher order regularity for the approximation of the flux function in the domain covered by the plasma, while preserving accurate meshing of the geometric details in the rest of the computational domain and simplifying the inclusion of ferromagnetic parts.

1 Introduction

Theoretical and computational plasma physics is a wide subject with applications ranging from low temperature plasmas for lighting, thrusters and materials processing to hot plasmas for fusion; from ultra-cold plasmas to particle accelerators; from beams to pulsed power; and from intense kinetic nonequilibrium plasmas to high power microwaves. Each application is characterized by a proper space-time scaling, mathematical model and computational approach. In this work, we are interested in simulating the equilibrium of a plasma for fusion reaction in a tokamak [3]. We propose a finite element approach involving highly regular approximations of the magnetic flux field on a triangular mesh of the tokamak poloidal section. Differently to other approaches in the recent literature (see for example [9, 10, 11]), to solve

Francesca Rapetti · Blaise Faugeras · Cedric Boulbe
Dép. de Mathématiques, Univ. Côte d'Azur, CNRS, INRIA Med. (Castor Team), Nice (FR). e-mail: francesca.rapetti, blaise.faugeras, cedric.boulbe at univ-cotedazur.fr
This work is supported by the French National Res. Agency (ANR-19-CE46-0005-03).

the axisymmetric formulation of the free-boundary plasma equilibrium in a tokamak, we rely on a non-conforming domain decomposition approach that couples piece-wise linear finite elements in a region that does not contain the plasma and reduced Hsieh-Clough-Tocher [5] finite elements elsewhere. This approach gives the flexibility to achieve easily and at low cost higher order regularity for the approximation of the flux function in the domain covered by the plasma, while preserving accurate meshing of the geometric details in the rest of the computational domain and simplifying the inclusion of ferromagnetic parts. The continuity of the numerical solution at the coupling interface is weakly enforced by mortar projection [2]. This work generalizes the method proposed in [6] to compute a plasma equilibrium in tokamak devices that include nonlinear ferromagnetic materials. To underline the differences with the iron-free case in terms of the poloidal magnetic induction distribution and of the Newton algorithm convergence, we suppose that the iron parts occupy all the exterior part of the WEST or JET tokamaks so that it is possible to remain within an axisymmetric formulation. Indeed, a correct treatment of the iron case¹ would necessitate a full three-dimensional computation of the plasma equilibrium that goes beyond the purpose of the present work. Numerical simulations are here performed with the software NICE (see [7]).

2 The direct static equilibrium problem

In a *plasma* for nuclear fusion, the charged particles (essentially, tritium and deuterium) at an extremely high temperature (ten times larger than that in the Sun) endure a fusion reaction, that is they stich together, against the Coulomb repulsion, yielding production of energy, helium and neutrons. No

¹ The choice of an iron-transformer tokamak is due to Paul-Henri Rebut, a French physicist, working on nuclear fusion. From 1970 to 1973, Rebut contributed to the creation of TFR (Tokamak of Fontenay-aux-Roses), then of JET (Joint European Torus) and of Tore Supra, that later became WEST (Tungsten (W) Environment in Steady-state Tokamak). In a tokamak with iron, the magnetic field lines are better conveyed (than by the air) leading to an increase in the poloidal flux thus generating a longer fusion reaction (at that time, the technology of supraconducting coils to generate high intensity fields was not so well developed yet). However, the presence of the iron makes numerical computations more involved. Indeed, the magnetic permeability μ depends non linearly on the magnetic induction and the Green function, that relates directly the magnetic flux to the generating currents in an iron-free tokamak, cannot be used anymore. Moreover, the presence of iron parts (an internal kernel with an arm) breaks the toroidal symmetry of the physical parameter distribution despite the plasma equilibrium is an axisymmetric phenomenon. On the top of this, for the TFR, the presence of iron caused an instability on the horizontal displacement of the plasma [12, 4]. Tokamaks of new generation, such as ITER, are iron-free: thanks to modern technologies, the magnetic induction in the plasma can easily reach 10 teslas (and this would have not been possible with iron parts saturating at lower intensities).

material on Earth can support the temperature of such a hot mixture but due to the fact that the involved particles are charged, they can be confined in a toroidal chamber with magnetic field, *tokamak* in Russian. An additional iron structure can be installed in a tokamak to increase the poloidal flux thus generating a longer reaction. To keep up a fusion reaction we have, among many other tasks, to control the plasma in order to maintain it in equilibrium. A comprehensive survey of the (direct and inverse) mathematical problems associated with this equilibrium and of their low-order finite element modeling is described in [8] and the therein references. Here, we focus on the direct problem of computing a static equilibrium of a plasma in a tokamak by high-order finite elements. We thus work at the diffusion time scale (the slowest one) in a device with characteristic length of meters and suppose to eliminate all terms containing a time derivative in the kinetic and magnetic equations. The equations describing such an equilibrium are respectively, force balance (between the kinetic force and the magnetic part of the Lorentz force), Ampère theorem and the solenoidal condition, that read

$$\text{grad } p = \mathbf{J} \times \mathbf{B}, \quad \text{curl} \frac{1}{\mu} \mathbf{B} = \mathbf{J}, \quad \text{div} \mathbf{B} = 0, \quad (1)$$

where p (with dimensions in the SI system² as $[M][L]^{-1}[T]^{-2}$) is the plasma kinetic pressure, \mathbf{B} (as $[M][T]^{-2}[I]^{-1}$) is the magnetic induction field, \mathbf{J} (as $[I][L]^{-2}$) is the current density and μ (as $[M][L][T]^{-2}[I]^{-2}$) the magnetic permeability. Under the assumption of perfect axial symmetry of the device geometry and physical parameters' distribution, we reformulate (1) in cylindrical coordinates (r, φ, z) and work in a poloidal section ($\phi = C$) of the tokamak. The primal unknown is the poloidal magnetic flux $\psi = r \mathbf{A} \cdot \mathbf{e}_\varphi$, namely the scaled toroidal component of the vector potential \mathbf{A} , with $\mathbf{B} = \text{curl} \mathbf{A}$ and \mathbf{e}_φ the unit vector for the ϕ coordinate. The poloidal magnetic flux ψ is a key quantity in modeling plasma in tokamaks as the lines of both the current density \mathbf{J} and magnetic induction \mathbf{B} lie on surfaces of constant value for such a flux, the so-called *magnetic surfaces* (see [3] for more details). These are closed nested surfaces, that do not intersect with any material of the tokamak, and ensure the confinement of charged particles hence the confinement of plasma inside a tokamak.

We introduce $\mathcal{D} = [0, \infty] \times [-\infty, \infty]$, the positive half plane that contains the poloidal section. Equations (1) in \mathcal{D} becomes

$$-\partial_r \left(\frac{1}{\mu(\psi)r} \partial_r \psi \right) - \partial_z \left(\frac{1}{\mu(\psi)r} \partial_z \psi \right) := -\Delta^* \psi = J_\varphi \quad (2)$$

in coordinates (r, φ, z) , where $J_\varphi \mathbf{e}_\varphi$ is the toroidal component of \mathbf{J} . The geometry of the tokamak determines various subdomains (see Fig. 1, left) that

² In the Standard International (SI) unit system, mass M (kg), length L (m), time T (s) and current intensity I (A) are base dimensions (resp., units).

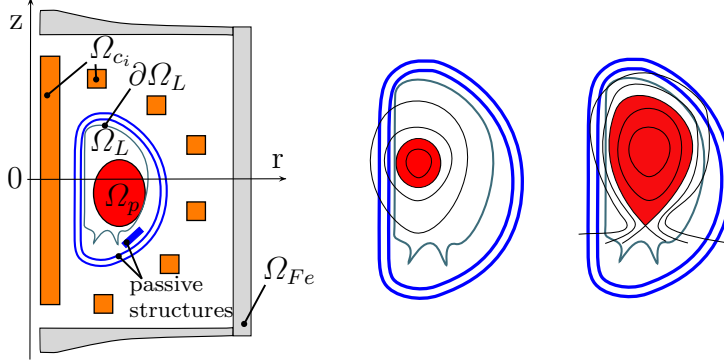


Fig. 1 Left: Geometric description of the tokamak in the poloidal plane. Middle and right, sketch for characteristic plasma shapes. The plasma boundary touches the limiter or the plasma is enclosed by a flux line that goes through an X-point.

are used to set J_φ accordingly. In these pages, passive structures are not modeled (they are hence supposed to be characterised by an electric conductivity $\sigma = 0$). We have:

- $\Omega_{Fe} \subset \mathcal{D}$ denotes those parts of \mathcal{D} made of iron where the permeability μ is not constant and given as a (non-linear) function of ψ , namely $\mu(\psi) = \mu_{Fe}(|\nabla\psi|^2 r^{-2})$; if $\Omega_{Fe} = \emptyset$, then $\mu = \mu_0$ everywhere;
- $\Omega_{c_i} \subset \mathcal{D}$, $1 \leq i \leq N_c$, denotes the intersection of the i th coil with the poloidal plane. We suppose that the i th coil cross section area is $|\Omega_{c_i}|$, with total current I_i ;
- $\Omega_L \subset \mathcal{D}$, denotes the domain bounded by the limiter, thus the domain accessible by the plasma;
- $\Omega_p \subset \Omega_L$, denotes the domain covered by the plasma and the boundary $\partial\Omega_p$ is the outermost closed ψ -isocontour contained within Ω_L .

The static direct equilibrium problem thus reads: find ψ such that

$$-\Delta^* \psi = \begin{cases} rp'(\psi) + \frac{1}{\mu_0 r} ff'(\psi) & \text{in } \Omega_p(\psi), \\ I_i(\psi)/|\Omega_{c_i}| & \text{in } \Omega_{c_i}, \quad i = 1, N_c, \\ 0 & \text{elsewhere,} \end{cases} \quad (3)$$

$$\psi(0, z) = 0, \quad \lim_{\|(r,z)\| \rightarrow +\infty} \psi(r, z) = 0.$$

The first line of (3), stated in the plasma domain, is the celebrated Grad-Shafranov-Schlüter equation [13]. The plasma domain $\Omega_p(\psi)$ is unknown and depends non-linearly on the poloidal flux ψ (we have a free-boundary problem). The boundary of $\Omega_p(\psi)$ either touches that of Ω_L (limiter configuration, as in Fig. 1 middle) or contains one or more saddle points of ψ (divertor configuration, as in Fig. 1 right). The saddle points of ψ , denoted by $(r_X, z_X) = (r_X(\psi), z_X(\psi))$, are called X-points of ψ . The plasma domain

$\Omega_p(\psi)$ is the largest subdomain of Ω_L bounded by a closed ψ -isoline in Ω_L and containing the magnetic axis (r_a, z_a) . The magnetic axis is the point $(r_a, z_a) = (r_a(\psi), z_a(\psi))$, where ψ has its global maximum (or minimum, depending on axis positive direction) in Ω_L . Let $(r_b, z_b) = (r_b(\psi), z_b(\psi))$ be the point that determines the plasma boundary. Note that (r_b, z_b) is either an X-point of ψ or the contact point with $\partial\Omega_L$. The domain of p' and $f f'$ is the interval $[\psi_a, \psi_b]$ (supposing $\psi_a < \psi_b$) with the scalar values ψ_a and ψ_b being the flux values at the *magnetic axis* and at the boundary of the plasma. Since the domain of p' and $f f'$ depends on the poloidal flux itself, it is more practical to supply these profiles as functions of the normalized poloidal flux $\psi_N(r, z) = (\psi(r, z) - \psi_a(\psi)) / (\psi_b(\psi) - \psi_a(\psi))$. These two functions, subsequently termed $S_{p'}$ and $S_{f f'}$, have, independently of ψ , a fixed domain $[0, 1]$ (see [3] for more details on these functions). To solve numerically problem (3) we need to work in a domain $\Omega \subset \mathcal{D}$, known as the ABB domain [1] associated with \mathcal{D} (see Fig. 2, left), delimited by a *semi-circle* γ of radius $\rho_\gamma > 0$ including $\Omega_L \cup \Omega_{Fe} \cup_i \Omega_{ci}$ and the vertical *segment* $\Gamma_0 = \{0\}_r \times [-\rho_\gamma, \rho_\gamma]_z$.

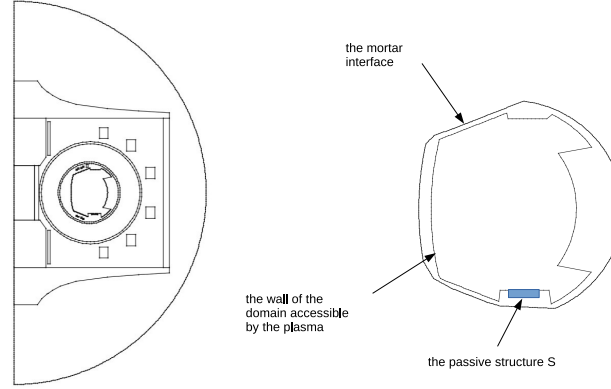


Fig. 2 The ABB domain (left) associated with \mathcal{D} and a zoom (right) on the subdomain Ω^{in} involved in the domain decomposition formulation. The mortar interface \mathcal{I} appears on the right but not on the left, as it is not a physical one. The passive structure S is drawn for completeness but its modeling is not considered here.

Here comes the non-overlapping domain decomposition framework. We set $\Omega = \Omega^{\text{in}} \cup \Omega^{\text{ex}}$ where Ω^{in} is a bounded domain containing Ω_L (see Fig. 2, right) and $\Omega^{\text{ex}} = \Omega \setminus \Omega^{\text{in}}$. The boundary of Ω^{in} is denoted \mathcal{I} , to recall that it is an interface between the two subdomains Ω^{in} , Ω^{ex} , on which we will impose the continuity of ψ , in a weak sense, through a mortar-like L^2 projection [2]. The weak formulation of (3) is: Find $\psi = (\psi_{\text{ex}}, \psi_{\text{in}}) \in \mathcal{V}$ such that

$$a(\psi, s) := a^{\text{ex}}(\psi_{\text{ex}}, v) + a^{\text{in}}(\psi_{\text{in}}, w) = \ell(I, s) \quad \forall s = (v, w) \in \mathcal{V}_{0, \mathcal{I}} \quad (4)$$

where $\mathcal{V} = \{(v, w) \in \mathcal{H}^1(\Omega^{\text{ex}}) \times \mathcal{H}^1(\Omega^{\text{in}}), v|_{\gamma_0} = 0, v|_{\mathcal{I}} = w|_{\mathcal{I}}\}$, being $\mathcal{H}^1(\Omega) = \{u \in L_*^2(\Omega), \nabla u \in L_*^2(\Omega)^2\}$ with $L_*^2(\Omega) = \{g : \Omega \rightarrow \mathbb{R}, \|g\|_{*, \Omega}^2 :=$

$\int_{\Omega} g^2 \frac{1}{r} dr dz < \infty$. We have also set $\mathcal{V}_{0,\mathcal{I}} = \{(v, w) \in \mathcal{V}, v|_{\mathcal{I}} = w|_{\mathcal{I}} = 0\}$ and

$$\begin{aligned} a^{\text{ex}}(\psi, v) &:= \int_{\Omega^{\text{ex}}} \frac{1}{\mu r} \nabla \psi \cdot \nabla v dr dz + c(\psi, v), \\ a^{\text{in}}(\psi, w) &:= \int_{\Omega^{\text{in}}} \frac{1}{\mu_0 r} \nabla \psi \cdot \nabla w dr dz - J_p(\psi, w), \\ J_p(\psi, w) &:= \int_{\Omega_p(\psi)} \left(\frac{r}{r_0} \mathcal{A}(\psi_N) + \frac{r_0}{r} \mathcal{B}(\psi_N) \right) w dr dz, \\ \ell(I, s) &:= \sum_{i=1}^{N_c} \frac{I_i}{|\Omega_{c_i}|} \int_{\Omega_{c_i}} (\chi_{\Omega^{\text{ex}}} v + \chi_{\Omega^{\text{in}}} w) dr dz \end{aligned} \quad (5)$$

with, respectively, r_0 the characteristic radius (in meters) of Ω_L , λ a scaling coefficient such that the total plasma current is $I_p = \lambda J_p$, the functions \mathcal{A}, \mathcal{B} parametric representations of $S_{p'}$, $S_{ff'}$, and $\mu = g(\frac{|\nabla \psi|^2}{r^2}) \chi_{\Omega_{Fe}} + \mu_0 \chi_{\Omega^{\text{ex}} \setminus \Omega_{Fe}}$ in the expression of $a^{\text{ex}}(\psi, v)$ (here, χ_D is the characteristic function of a set D). We assume that the function g , defining μ in Ω_{Fe} , is known. In practical applications μ needs to be estimated from experimental data. Note that $\ell(I, s)$ contains the expression $\chi_{\Omega^{\text{ex}}} v + \chi_{\Omega^{\text{in}}} w$ to deal with the presence of coils in Ω^{in} and Ω^{ex} . Moreover, $c(\psi, v) \approx \int_{\partial \Omega} v \partial_n \psi d\Gamma$ to take into account the condition at infinity on γ , namely $\lim_{r \rightarrow 0^+} \int_{\{r\} \times [-\rho_\gamma, \rho_\gamma] \cap \Omega} \psi(r, z)^2 \frac{1}{r^2} dz = 0$. Under suitable assumptions, such as for example $\Omega_{Fe} = \emptyset$ or $J_p(\cdot)$ assigned, it can be proved that problem (4) has a unique solution but in the general case the question is theoretically open. In the next section, we propose a Newton method to solve the discrete problem associated with (4) when $\Omega_{Fe} \neq \emptyset$. To define the corresponding Jacobian matrix, we first compute the derivatives w.r.t. the unknown field ψ of the non-linear operators in (4), and then we evaluate them on discrete fields with special care. By relying on directional derivatives, we can compute $D_\psi a^{\text{ex}}(\cdot, \cdot)$ as follows

$$D_\psi a^{\text{ex}}(\psi, s)(\tilde{\psi}) = a^{\text{ex}}(\tilde{\psi}, s) - 2 \int_{\Omega_{Fe}} \frac{g'(\cdot)}{g^2(\cdot)} \frac{1}{r^3} (\nabla \tilde{\psi} \cdot \nabla \psi) (\nabla \psi \cdot \nabla s). \quad (6)$$

For $D_\psi a^{\text{in}}(\cdot, \cdot)$, the derivative w.r.t. ψ of $J_p(\cdot, \cdot)$ is computed analytically on an approximation of this functional by a quadrature formula³.

3 A Newton method for the discrete problem

Let τ^{ex} (resp. τ^{in}) be a mesh of triangles that covers Ω^{ex} (resp. Ω^{in}). The two meshes $\tau^{\text{ex}}, \tau^{\text{in}}$ are shape regular and quasi-uniform, with maximal diameters $h_{\text{ex}}, h_{\text{in}}$, respectively. We assume that \mathcal{I} is a polygonal with nodes and edges in τ^{ex} . We wish to use in $\Omega_L \subset \Omega^{\text{in}}$, a finite element approximation ψ_h for the poloidal flux ψ that is not only continuous but has also

³ To approximate $J_p(\cdot, \cdot)$ in (5) by a quadrature formula we need to know the domain $\Omega_p(\psi)$ occupied by the plasma. This domain is an unknown of the equilibrium problem, as it depends on ψ . An efficient technique to determine it is stated in [6].

component-wise continuous gradient $\nabla\psi_h$. This is possible if we use the reduced or minimal Hsieh-Clough-Tocher (rHCT) finite element space, say \mathcal{V}^{in} , on τ^{in} (see [5]). This regularity is not necessary in Ω^{ex} therefore we couple rHCT finite elements in Ω^{in} with continuous piece-wise linear finite elements, say \mathcal{V}^{ex} , on τ^{ex} . Note that $\Omega_{Fe} \subset \Omega^{\text{ex}}$. Let us also write $\mathcal{V}^{\text{ex}} = \mathcal{V}_\circ^{\text{ex}} \oplus \mathcal{E}\mathcal{V}_\partial^{\text{ex}}$ and $\mathcal{V}^{\text{in}} = \mathcal{V}_\circ^{\text{in}} \oplus \mathcal{E}\mathcal{V}_\partial^{\text{in}}$, where, for example, $\mathcal{V}_\circ^{\text{ex}}$ (resp. $\mathcal{V}_\partial^{\text{ex}}$) is the subspace of \mathcal{V}^{ex} described by basis functions associated with dofs at nodes in $\bar{\Omega}^{\text{ex}} \setminus \mathcal{I}$ (resp., $\bar{\Omega}^{\text{ex}} \cap \mathcal{I}$) and \mathcal{E} denotes the corresponding trivial extension operator. The functions in $\mathcal{V}_\circ^{\text{ex}}$ and $\mathcal{V}_\circ^{\text{in}}$ have vanishing Dirichlet trace on \mathcal{I} . The discrete problem to solve reads: Find $\psi_h \in \mathcal{V}_h$ such that

$$a(\psi_h, s_h) = \ell(I, s_h) \quad \forall s_h = (v_h, w_h) \in \mathcal{V}_\circ^{\text{ex}} \times \mathcal{V}_\circ^{\text{in}} \quad (7)$$

where $\mathcal{V}_h = \{(u_h^{\text{in}}, u_h^{\text{ex}}) \in \mathcal{V}^{\text{in}} \times \mathcal{V}^{\text{ex}}, u_h^{\text{ex}}|_{\gamma_0} = 0, \int_{\mathcal{I}} (u_h^{\text{in}} - u_h^{\text{ex}}) z_h d\mathcal{I} = 0, \forall z_h \in \mathcal{M}_h\}$, with $\mathcal{M}_h = \{\xi_h \in \mathcal{C}^0(\mathcal{I}) : \xi_h|_e \in \mathbb{P}_1(e), \forall e \in (\tau^{\text{ex}})|_{\mathcal{I}}\}$ the mortar multiplier space. The bilinear and linear forms $a(\cdot, \cdot)$, $\ell(I, \cdot)$ are defined as for the problem (4) and evaluated in (7) for functions in the discrete space \mathcal{V}_h .

Let us denote by $\{v_i^{\text{ex}}\}_{i=1, N^{\text{ex}}}$ the dual basis of \mathcal{V}^{ex} for the P1 dofs associated with the N^{ex} nodes $V_i \in \tau^{\text{ex}}$ and $\{w_j^{\text{in}}\}_{j=1, 3N^{\text{in}}}$ that of \mathcal{V}^{in} for the rHCT dofs at the N^{in} nodes $V_j \in \tau^{\text{in}}$. Let \mathbf{A} (resp. \mathbf{C} , \mathbf{L}^{in} , \mathbf{L}^{ex}) be the matrix associated with the integral expressions in (5) contained in $a(\cdot, \cdot)$ (resp., in $c(\cdot, \cdot)$, in $\ell(\cdot, \cdot)$ for the coil Ω_{c_i} if this coil is in Ω^{in} or in Ω^{ex}) and $\mathbf{J}(\cdot)$ (resp., \mathbf{U}_I^{in} , \mathbf{U}_I^{ex}) the vector with components resulting from $\mathbf{J}_p(\cdot)$ (resp., holding the currents I_i for the coil Ω_{c_i} if it is in Ω^{in} or in Ω^{ex}). To take into account iron parts in Ω^{ex} , we separate the elliptic operator into the linear part and a nonlinear part, say $\mathbf{A}_0\boldsymbol{\psi} + \mathbf{A}_\mu(\boldsymbol{\psi})$, where the vector $\boldsymbol{\psi}$ gathers all dofs of $\psi_h \in \mathcal{V}_h$, the matrix \mathbf{A}_0 has entries $(\mathbf{A}_0)_{ij} = \int_{\Omega^{\text{ex}} \setminus \Omega_{Fe}} \frac{1}{\mu_0 r} \nabla v_i^{\text{ex}} \cdot \nabla v_j^{\text{ex}} dr dz$ and the vector $\mathbf{A}_\mu(\boldsymbol{\psi})$ has components $\mathbf{A}_{\mu, i}(\boldsymbol{\psi}) = \int_{\Omega_{Fe}} \frac{1}{\mu(\psi_h)r} \nabla v_i^{\text{ex}} \cdot \nabla \psi_h dr dz$, being $i, j = 1, N^{\text{ex}}$. Equation (7) in its fully discretized form reads $\mathbf{e}(\boldsymbol{\psi}) = \mathbf{0}$ with

$$\mathbf{e}(\boldsymbol{\psi}) := (\mathbf{A}_0 + \mathbf{C})\boldsymbol{\psi} + \mathbf{A}_\mu(\boldsymbol{\psi}) - \mathbf{J}(\boldsymbol{\psi}) - \mathbf{L}^{\text{in}} \mathbf{U}_I^{\text{in}} - \mathbf{L}^{\text{ex}} \mathbf{U}_I^{\text{ex}} \quad (8)$$

where, for $k = 1, 3N^{\text{in}}$, we have

$$(\mathbf{J}(\boldsymbol{\psi}))_k = \int_{\Omega_p(\psi_h)} \mathbf{J}_p(\psi_{N, h}, r) w_k dr dz, \quad \text{and} \quad \mathbf{L}_{i, k}^{\text{in}} = \frac{1}{|\Omega_{c_i}|} \int_{\Omega_{c_i}} w_k^{\text{in}} dr dz,$$

for those indices $i = 1, N_c$ such that $\Omega_{c_i} \subset \Omega^{\text{in}}$. For the indices i such that $\Omega_{c_i} \subset \Omega^{\text{ex}}$, the definition of $\mathbf{L}_{i, j}^{\text{ex}}$, with $j = 1, N^{\text{ex}}$, is similar to that of $\mathbf{L}_{i, k}^{\text{in}}$, just replacing w_k^{in} by v_j^{ex} . Newton iterations for problem (8) are

$$\boldsymbol{\psi}^{n+1} = \boldsymbol{\psi}^n - [\mathbf{e}_\psi(\boldsymbol{\psi}^n)]^{-1} \mathbf{e}(\boldsymbol{\psi}^n), \quad [\mathbf{e}_\psi(\boldsymbol{\psi})] = D_\psi [(\mathbf{A}_0 + \mathbf{C})\boldsymbol{\psi} + \mathbf{A}_\mu(\boldsymbol{\psi})] - D_\psi \mathbf{J}(\boldsymbol{\psi}).$$

Let \mathbf{u}^{ex} and \mathbf{u}^{in} gather the values of dofs for $\psi_h^{\text{ex}} \in \mathcal{V}^{\text{ex}}$ and $\psi_h^{\text{in}} \in \mathcal{V}^{\text{in}}$, respectively. We have $\mathbf{u}^{\text{ex}} = (\mathbf{u}_\circ^{\text{ex}}, \mathbf{u}_\partial^{\text{ex}})$ and $\mathbf{u}^{\text{in}} = (\mathbf{u}_\circ^{\text{in}}, \mathbf{u}_\partial^{\text{in}})$ where $\mathbf{u}_\circ^{\text{ex}}$ (resp.

\mathbf{u}_o^{in} and $\mathbf{u}_\partial^{\text{ex}}$ (resp. $\mathbf{u}_\partial^{\text{in}}$) are for dofs in V_o^{ex} (resp. V_o^{in}) and V_∂^{ex} (resp. V_∂^{in}). The mortar coupling condition in \mathcal{V}_h links the block $\mathbf{u}_\partial^{\text{ex}}$ to the block $\mathbf{u}_\partial^{\text{in}}$ by the matrix relation $\mathbf{P}\mathbf{u}_\partial^{\text{ex}} = \mathbf{D}\mathbf{u}_\partial^{\text{in}}$ with $(\mathbf{P})_{i,j} = \int_{\mathcal{I}} v_{\partial,i}^{\text{ex}} v_{\partial,j}^{\text{ex}} d\mathcal{I}$, for all $i, j = 1, N_\partial^{\text{ex}}$, and $(\mathbf{D})_{i,k} = \int_{\mathcal{I}} v_{\partial,i}^{\text{ex}} w_{\partial,k}^{\text{in}} d\mathcal{I}$, for all $i = 1, N_\partial^{\text{ex}}$ and $k = 1, N_\partial^{\text{in}}$. The inclusion of the coupling condition matrix form into the algebraic system associated with the discrete problem (7) is done by introducing the reduced variable, \mathbf{X} , such that

$$\boldsymbol{\psi} = \begin{pmatrix} \mathbf{u}_o^{\text{ex}} \\ \mathbf{u}_\partial^{\text{ex}} \\ \mathbf{u}_o^{\text{in}} \\ \mathbf{u}_\partial^{\text{in}} \end{pmatrix} = \begin{bmatrix} \mathbf{I} & 0 & 0 \\ 0 & 0 & \mathbf{P}^{-1}\mathbf{D} \\ 0 & \mathbf{I} & 0 \\ 0 & 0 & \mathbf{I} \end{bmatrix} \begin{pmatrix} \mathbf{u}_o^{\text{ex}} \\ \mathbf{u}_\partial^{\text{in}} \\ \mathbf{u}_\partial^{\text{in}} \end{pmatrix} = \mathbf{Q}\mathbf{X}.$$

Equation (8) rewritten in terms of \mathbf{X} becomes

$$\mathbf{e}(\mathbf{X}) := \mathbf{Q}^\top [(\mathbf{A}_0 + \mathbf{C})\mathbf{Q}\mathbf{X} + \mathbf{A}_\mu(\boldsymbol{\psi}) - \mathbf{J}(\boldsymbol{\psi}) - \mathbf{L}^{\text{in}}\mathbf{U}_I^{\text{in}} - \mathbf{L}^{\text{ex}}\mathbf{U}_I^{\text{ex}}]. \quad (9)$$

For $\mathbf{J}(\boldsymbol{\psi}) = \mathbf{J}(\mathbf{Q}\mathbf{X}) = \mathbf{H}(\mathbf{X})$ we get $D_{\mathbf{X}}\mathbf{H}(\mathbf{X})d\mathbf{X} = D_{\boldsymbol{\psi}}\mathbf{J}(\boldsymbol{\psi})\mathbf{Q}d\mathbf{X} = \text{Jac}_{\boldsymbol{\psi}}(\boldsymbol{\psi})\mathbf{Q}d\mathbf{X}$, and for $\mathbf{A}_\mu(\boldsymbol{\psi}) = \mathbf{A}_\mu(\mathbf{Q}\mathbf{X}) = \mathbf{G}(\mathbf{X})$, we obtain $D_{\mathbf{X}}\mathbf{G}(\mathbf{X})d\mathbf{X} = \mathbf{A}_{\mu,\boldsymbol{\psi}}(\boldsymbol{\psi})\mathbf{Q}d\mathbf{X}$ with $[\mathbf{A}_{\mu,\boldsymbol{\psi}}]_{i,j}$ given in (6) by setting $\psi_h, v_i^{\text{ex}}, v_j^{\text{ex}}$ at the place of $\psi, \tilde{\psi}$ and s , respectively. Newton iterations for problem (9) read

$$\mathbf{X}^{n+1} = \mathbf{X}^n - [\mathbf{e}_{\mathbf{X}}(\mathbf{X}^n)]^{-1} \mathbf{e}(\mathbf{X}^n) \quad (10)$$

where $[\mathbf{e}_{\mathbf{X}}(\mathbf{X}^n)] = \mathbf{Q}^\top [(\mathbf{A}_0 + \mathbf{C}) + \mathbf{A}_{\mu,\boldsymbol{\psi}}(\boldsymbol{\psi}^n) - \text{Jac}_{\boldsymbol{\psi}}(\boldsymbol{\psi}^n)]\mathbf{Q}$. In the next section, we present some numerical results.

4 Numerical results

It does not exist, to our knowledge, analytical solutions for the free-boundary equilibrium problem considered in this paper. We provide nevertheless some numerical evidence of convergence for the proposed method.

The initial guess of the plasma domain $\Omega_p(\psi)$ for given currents in the poloidal field coils plays a crucial role in free-boundary equilibrium problems. Here, we find such initial guesses by solving inverse problems or optimal control problems, where a desired shape and position of the plasma domain is the objective and the precise values of the currents is unknown. In the present case we do not focus on this technical issue, but assume we have a good initial guess for the poloidal flux from, e.g., a non-mortar formulation of the free-boundary equilibrium problem involving P1 FEs everywhere, as explained in [7]. Then, the good convergence of the Newton iterations applied to (9) is shown in Table 1. We remark that the presence of iron parts slows down considerably the convergence speed.

n	if $\Omega_{Fe} = \emptyset$	if $\Omega_{Fe} \neq \emptyset$
1	1.77919×10^{-2}	9.78267×10^{-3}
2	4.35470×10^{-4}	8.56241×10^{-4}
3	4.05152×10^{-7}	6.17721×10^{-4}
4	2.80505×10^{-11}	3.46301×10^{-4}
5		9.38432×10^{-5}
6		3.09165×10^{-5}
7		8.76154×10^{-6}
8		3.11734×10^{-6}
9		5.16426×10^{-7}
10		2.58976×10^{-10}
11		6.29602×10^{-14}

Table 1 Convergence history of Newton iterations for WEST: iteration number n and residual relative error $\|\mathbf{X}^n - \mathbf{X}^{n-1}\|/\|\mathbf{X}^{n-1}\|$, with either $\Omega_{Fe} = \emptyset$ or $\Omega_{Fe} \neq \emptyset$.

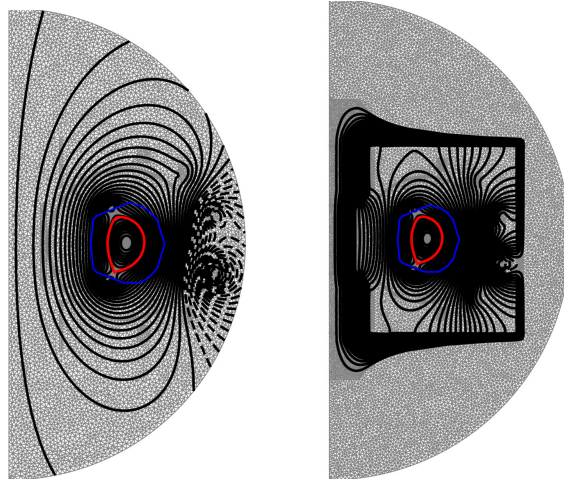


Fig. 3 Magnetic flux isolines in the poloidal section of WEST, supposing either $\Omega_{Fe} = \emptyset$ (left) or $\Omega_{Fe} \neq \emptyset$ (right).

Fig. 3 shows a typical WEST poloidal flux map calculated by NICE. A zoom on the distribution of ψ_h in Ω^{in} is proposed in Fig. 4, for the case $\Omega_{Fe} \neq \emptyset$. The X-point and plasma axis are enlightened in the small pictures. With high-order FEs in Ω^{in} , these points do not coincide with nodes of the computational mesh, as it would be the case with P1 FEs, thus assuming a more physically meaningful position.

References

1. R. ALBANESE, J. BLUM, O. BARBIERI. *On the solution of the magnetic flux equation in an infinite domain*. In Proc. of the 8th Europhysics Conference on

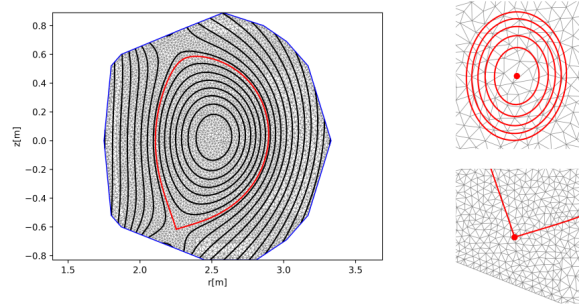


Fig. 4 Magnetic flux isolines in Ω^{in} (left), together with a zoom around the plasma axis (right, top) and X-point (right, bottom).

- Computing in Plasma Physics (1986) 41–44.
2. C. BERNARDI, Y. MADAY, A.T. PATERA. *A new nonconforming approach to domain decomposition: The mortar element method*. In *Nonlinear Partial Differential Equations and Their Applications*. in H. Brézis and J.-L. Lions (eds.), Collège de France Seminar XI., 1992.
 3. J. BLUM, *Numerical Simulation and Optimal Control in Plasma Physics with Applications to Tokamaks*. Series in Modern Applied Mathematics. Wiley Gauthier-Villars, Paris, 1989.
 4. J. BLUM, J. LE FOLL, B. THOORIS. *The self-consistent equilibrium and diffusion code SCED*. *Comp. Phys. Communications* 24 (1981) 235–254.
 5. R.W. CLOUGH, J.L. TOCHER. *Finite element stiffness matrices for analysis of plates in bending*. In *Proc. Conf. Matrix Methods in Struct. Mech.*, Air Force Inst of Tech., Wright Patterson A.F Base, Ohio, October 1965.
 6. A. ELARIF, B. FAUGERAS, F. RAPETTI. *Tokamak free-boundary plasma equilibrium computation using finite elements of class C^0 and C^1 within a mortar element approach*. *J. Comput. Phys.* 439 (2021) 110388.
 7. B. FAUGERAS. *An overview of the numerical methods for tokamak plasma equilibrium computation implemented in the NICE code*. *Fusion Eng. Design*, 160:112020, 2020.
 8. H. HEUMANN, J. BLUM, C. BOULBE, B. FAUGERAS, G. SELIG, J.-M. ANÉ, S. BRÉMOND, V. GRANGIRARD, P. HERTOUT, E. NARDON. *Quasi-static free-boundary equilibrium of toroidal plasma with CEDRES++: computational methods and applications*. *J. Plasma Physics* 81 (2015) 905810301.
 9. H. HEUMANN, F. RAPETTI, *A finite element method with overlapping meshes for free-boundary axisymmetric plasma equilibria in realistic geometries*. *J. Comput. Phys.* 334 (2017) 522–540.
 10. S. MINJEAUD, R. PASQUETTI. *Fourier-spectral elements approximation of the two fluid ion-electron Braginskii system with application to tokamak edge plasma in divertor configuration*. *J. Comput. Phys.* 321 (2016) 492–511.
 11. A. RATNANI, N. CROUSEILLES, E. SONNENDRÜCKER. *An Isogeometric Analysis Approach for the study of the gyrokinetic quasi-neutrality equation*. *J. Sci. Comput.* 231 (2012) 373–393.
 12. P.H.REBUT. *Instabilités non magnétohydrodynamiques dans les plasmas à densités de courant élevé*. *J. Nuclear Energy Part C*, 4 (1963) 159.
 13. V.D. SHAFRANOV. *On magnetohydrodynamical equilibrium configurations*. *Sov. J. Exper. Theoret. Phys.* 6 (1958) 545.